

AD/A-005 589

THE UTILIZATION OF STARUTE DECELERATORS FOR IMPROVED UPPER ATMOSPHERE MEASUREMENTS

R. O. Olsen, et al

Army Electronics Command
Fort Monmouth, New Jersey

December 1974

DISTRIBUTED BY:

NTIS

National Technical Information Service
U. S. DEPARTMENT OF COMMERCE

NOTICES

ACCESSION FOR	
NTIS	White Section <input checked="" type="checkbox"/>
DDC	Buff Section <input type="checkbox"/>
UNANNOUNCED	<input type="checkbox"/>
JUSTIFICATION.....	
BY.....	
DISTRIBUTION/AVAILABILITY CODES	
Dist.	AVAIL. and/or SPECIAL
A	

Disclaimers

The findings in this report are not to be construed as an official Department of the Army position, unless so designated by other authorized documents.

The citation of trade names and names of manufacturers in this report is not to be construed as Official Government endorsement or approval of commercial products or services referenced herein.

Disposition

Destroy this report when it is no longer needed. Do not return it to the originator.

il

UNCLASSIFIED

SECURITY CLASSIFICATION OF THIS PAGE (When Data Entered)

REPORT DOCUMENTATION PAGE		READ INSTRUCTIONS BEFORE COMPLETING FORM	
1. REPORT NUMBER ECOM-5551	2. GOVT ACCESSION NO.	3. RECIPIENT'S CATALOG NUMBER AD/A-005589	
4. TITLE (and Subtitle) THE UTILIZATION OF STARUTE DECELERATORS FOR IMPROVED UPPER ATMOSPHERE MEASUREMENTS		5. TYPE OF REPORT & PERIOD COVERED	
		6. PERFORMING ORG. REPORT NUMBER	
7. AUTHOR(s) R. O. Olsen B. W. Kennedy		8. CONTRACT OR GRANT NUMBER(s)	
9. PERFORMING ORGANIZATION NAME AND ADDRESS Atmospheric Sciences Laboratory White Sands Missile Range, New Mexico 88002		10. PROGRAM ELEMENT, PROJECT, TASK AREA & WORK UNIT NUMBERS DA Task No. 1T765702D127-03	
11. CONTROLLING OFFICE NAME AND ADDRESS US Army Electronics Command Fort Monmouth, New Jersey 07703		12. REPORT DATE December 1974	
		13. NUMBER OF PAGES 28	
14. MONITORING AGENCY NAME & ADDRESS (if different from Controlling Office)		15. SECURITY CLASS. (of this report) Unclassified	
		15a. DECLASSIFICATION/DOWNGRADING SCHEDULE	
16. DISTRIBUTION STATEMENT (of this Report) Approved for public release; distribution unlimited.			
17. DISTRIBUTION STATEMENT (of the abstract entered in Block 20, if different from Report) DDC RECEIVED FEB 27 1975 REGISTRY D			
18. SUPPLEMENTARY NOTES PRICES SUBJECT TO CHANGE			
19. KEY WORDS (Continue on reverse side if necessary and identify by block number) 1. Sounding rockets 2. Decelerators 3. Upper Atmosphere 4. Research Meteorological Rockets			
20. ABSTRACT (Continue on reverse side if necessary and identify by block number) The results of flight tests of a 4.5-m-square Arcas Starute developed for upper atmosphere research are described. The development of this Starute evolved from the 2-m-square Loki Starute, a decelerator currently being used operationally for the Meteorological Rocket Network (MRN). The Arcas Starute possesses the following characteristics: low ballistic coefficient; deployment reliability at high altitudes; high stability;			

DD FORM 1 JAN 73 1473

Reproduced by
NATIONAL TECHNICAL
INFORMATION SERVICE
US Department of Commerce
Springfield VA 22151

UNCLASSIFIED

SECURITY CLASSIFICATION OF THIS PAGE (When Data Entered)

UNCLASSIFIED

SECURITY CLASSIFICATION OF THIS PAGE(When Data Entered)

20. Abstract (continued)

low angle of attack; and high radar reflectivity.

The Arcas Starute was deployed with different payload weights over a range of altitudes from 61 km to 78 km. In all cases the decelerator remained subsonic and proved to be extremely stable.

This paper discusses the environmental conditions under which decelerators are deployed from a research rocket, and the manner in which they are expected to perform when the deployment altitude varies from 61 km to 100 km. The Starute decelerator can improve the capabilities of upper air measurements by extending in situ wind sensing up to an altitude of 80 km. This device can be utilized for various atmospheric measurements which require subsonic velocities and a low angle of attack during sensing operations.

ia

UNCLASSIFIED

SECURITY CLASSIFICATION OF THIS PAGE(When Data Entered)

INTRODUCTION

The Meteorological Rocket Network (MRN), a cooperative effort by meteorological groups of the Army, Navy, Air Force, Atomic Energy Commission, National Oceanic and Atmospheric Administration, and National Aeronautics and Space Administration, provides upper atmospheric data above the heights attained by conventional balloon-borne radiosondes [1]. For many years routine soundings have been made with the Arcas rocket, a single stage meteorological rocket which carries telemetry payloads of approximately 1.4 to 1.8 kg to altitudes of 60 km to 80 km when launched at White Sands Missile Range, located at a launch elevation of 1.2 km MSL. The sounding system consists of the rocket vehicle, telemetry package, and sensor suspended below a decelerator. The decelerator usually has two functions: to decrease the fall rate of the sensor package to permit meaningful in situ measurements of upper atmosphere parameters, and to measure upper atmosphere winds as the parachute is tracked by radar during descent [2].

The requirements for meteorological rocketsonde decelerators are: (1) low ballistic coefficient, (2) deployment reliability, (3) acceptable stability, and (4) adequate radar cross section.

The Arcas hemisphere decelerator, used as a standard retardation device for many years, meets some of the criteria specified. However, a study [3] of the Arcas decelerator performance indicated that (1) the instability of the hemisphere configuration resulted in data dropouts in the telemetry records; (2) the decelerator descent rate is greater than desired over the portion of the trajectory of prime interest, above 45 km; and (3) there were variations from the predicted rate of descent.

Because of these undesirable qualities, investigations were conducted by ASL and NASA to define and perhaps eliminate some of the undesirable characteristics in decelerator performance. NASA Langley Research Center conducted tests by suspending an on-board camera from the parachute; in some cases, the film showed that the initial problems in proper deployment of the parachute were caused by shroud lines becoming tangled and twisted during the deployment sequence [4]. Also, data from ground-based cameras revealed that the parachutes were unstable, and the payloads exhibited a coning motion of approximately 45 degrees from the vertical at altitudes above 35 km (Figure 1).

The effect of a large coning motion of the suspended payload results in intermittent signal loss from the telemetry package due to the variation in antenna patterns between the transmitter and receiver. However, telemetry dropouts during the initial portion of the descent do not completely obscure meaningful data since they are of short duration, making it possible to extract the data manually. In some cases it has been noted that the telemetered rocketsonde temperature traces on an AN/GMD-1 radiosonde recorder exhibited an oscillatory characteristic concurrent with the telemetry dropouts

due to the bead thermistor sensor being alternately exposed to, and shaded from, direct solar radiation. The above makes it necessary to improve the existing decelerator and to develop other decelerators which could be utilized for meteorological sounding rocket applications. One of the efforts consisted of the development of the Ballute (balloon-parachute) decelerator by Goodyear Aerospace Corporation [5]. This type of decelerator uses entrapped air to inflate the Ballute envelope and ram air to maintain its configuration. These features eliminate one of the problems that other decelerator systems have at the higher altitudes: a lack of sufficient dynamic pressure to properly deploy the system. The Ballute has an inflated torus, called a "burble fence," which provides added stability, a highly desirable feature for a number of different types of high altitude atmospheric sensors. However, tests of the Arcas Ballute proved the system to be heavier than could be tolerated for meteorological rocketsonde applications, providing a ballistic coefficient slightly greater than the Arcas hemispheric parachute. Therefore, the only marked improvement over the operational system in use was in the Ballute system stability.

The smaller Loki Datasonde system (Figure 2) is currently widely used as an operational meteorological rocket for the MRN in lieu of the Arcas (Figure 3). The Datasonde system uses a 2-m-square decelerator known as a Starute (stable-parachute) (Figure 4), which is a smaller, modified version of the Arcas Ballute. In the Datasonde system configuration, the Starute exhibits excellent stability and fall rate characteristics, with telemetry dropouts being virtually eliminated due to the lower angle of attack. The slower fall rate improves its wind sensing capability, and the wind sensitivity altitude could be increased to near 80 km, well above the normal Loki Datasonde apogee which is nominally 65 to 70 km. The improved stability and lower angle of attack (deviation from the vertical) of the Starute can be advantageously applied to specialized payloads, since stability and low angles of attack (± 3 degrees) are very important in terms of scientific payloads which are flown on meteorological sounding rockets. One payload which would profit from utilizing the Starute is a Gerdien condenser which, to derive meaningful data, requires that the angle of attack be no greater than ± 10 degrees. Another type of payload which this decelerator should improve is the chemiluminescent ozonesonde, which is not as severely altitude-sensitive as the Gerdien condenser. However, the greater stability would aid in better defining the flow characteristics of the air sampled by the ozonesonde. In order to test the applicability of the Starute characteristics to other type payloads, a number of 45-m-square Starute decelerators were flight-tested on Arcas rockets at White Sands Missile Range (WSMR), New Mexico.

DESCRIPTION

The Starute is a decelerator that uses ram-air inflation pressure to

maintain its shape as it descends through the atmosphere. The inflation pressure is the result of ambient and dynamic pressure directed normal to the interior surface while the external ambient and dynamic pressure is directed obliquely. Therefore, the internal force is greater, insuring proper erection of the decelerator after deployment and during the descent phase.

The Starute configuration is square, as shown in Figure 4, with the attached burble fence providing improved stability, increased drag, and a means of positive inflation. Major Starute characteristics are presented in Table 1, and major dimensions are shown in Figure 5.

In the case of in situ measurements utilizing a Starute, the rocket payload is ejected from the rocket vehicle at apogee; as the Starute leaves the payload canister, it inflates by action of the entrapped air. The payload is suspended below the inlet by lines attached to the Starute body. The burble fence located at the equator of the Starute provides additional drag and acts to stabilize the decelerator by altering the flow about the Starute from a laminar to a turbulent flow. Vent openings are located between the main body of the Starute and the burble fence for the dual purpose of venting entrapped air during packaging and permitting the passage of air into and out of the burble fence, resulting in a positive inflation pressure without the possibility of overpressurizing the burble fence of the Starute. The burble fence is constructed from aluminized mylar to provide a good radar target.

The Starute configuration is well suited to high altitude research purposes because of its good stability, its low angle of attack ($+3^\circ$ from the vertical), and its ability to erect and maintain its shape at altitudes above 65 km. Usually measurements made on parachutes at these altitudes were restricted because of the insufficient dynamic pressure needed to deploy and erect the parachute. The higher deployment increased the likelihood of the parachute becoming tangled, since it tumbles a greater distance before enough pressure is available to erect the canopy. The problem of having a sufficient dynamic pressure to inflate the parachute for Arcas and Loki soundings can be seen in Figure 6. It indicates that a minimum force of 3.35 N/m^2 is required for full inflation. Figure 7 indicates the amount of horizontal velocity necessary for full decelerator inflation [6]. In the case of the Loki, the horizontal velocity at apogee is nominally 183 m/sec, when launched at elevation angles of between 78° and 86° . Figure 7 shows that inflation of a Loki parachute becomes marginal above 64 km. In the case of an Arcas rocket, where the nominal horizontal velocity is approximately 274 m/sec with similar elevation launch angles, the parachute exhibits marginal inflation characteristics above 70 km.

When a Starute is used in lieu of a parachute, the dynamic pressure for inflation is not required because residual air in the decelerator permits high altitude deployments. The limiting factor in terms of the Starute is

the stress placed on the material due to the differential pressures between the residual air in the Starute envelope and the ambient air at deployment.

A study of Starute decelerator descent characteristics with different payloads is based upon the theoretical ballistic coefficient, $M/C_d A$, and the deployment altitude. Here M is the combined mass of payload and parachute, C_d is the coefficient of drag, and A is the cross-sectional area of the decelerator. The equilibrium or terminal fall velocity of a decelerator is determined by its ballistic coefficient at the various altitudes, as shown in Figure 8. Figure 9 shows plots of the vertical velocity of several systems with different ballistic coefficients, and the terminal or equilibrium velocity for a particular ballistic coefficient. For a given specified deployment altitude, the ballistic coefficient determines dynamic overshoot velocity from the terminal velocity and from the altitude at which the system achieves terminal velocity. The vertical velocity increases and exceeds the equilibrium velocity for a period, and finally the velocity decreases to a point where the system is in equilibrium. High altitude deployment results in fall rates that are faster than the terminal velocity for the upper portion of the trajectory. At some altitude below the altitude at which that maximum velocity occurs the vertical velocity slows to the terminal velocity.

The amount that the vertical velocity exceeds the terminal velocity is dependent upon the ballistic coefficient, as shown in Figure 9. The junction of the two curves, terminal velocity and descent velocity, also indicates the altitude near which valid wind measurements can be made. This closely coincides in altitude to the point at which the meteorological rocket data have been empirically determined to be the maximum height of valid wind measurements. The criterion chosen is the altitude immediately below that of maximum descent velocity [7].

To further explore the utilization of the Starute as a high altitude decelerator, descent velocities were plotted (Figure 10) for various release altitudes and ballistic coefficients. Based on Figure 10 it appears that valid wind measurements can be made to 80 km when the decelerator possesses a ballistic coefficient of 0.048 kg/m^2 . From a practical sense it is desirable to keep the vertical velocity below the speed of sound because transonic and supersonic velocities degrade the atmospheric measurements. For example, the measurement of positive ion concentration with a blunt probe is more complex at supersonic velocities.

FLIGHT TESTS

All of the flight tests described in this study were made using Arcas rockets. Table 2 presents a summary of ten soundings. The first Arcas Starute was flown on 17 Sep 71; it failed because aerodynamic heating

fused together the mylar material, which was then ripped upon deployment. The aerodynamic heating problem was initially corrected by coating the parachute canister with an ablative material. In addition, an air gap and a reflective surface were provided to restrict the amount of heat that would be transferred to the Starute. The redesigned parachute package was flown on 2 Nov 71, and the Starute operated properly. For the next test on 6 Mar 71, the ablative coating was eliminated because it was a high cost item. This test was successful and proved that the ablative coating could be eliminated if an air gap and a reflective surface were placed between the canister wall and the Starute. Dimpled steel staves covered with aluminum tape provided adequate protection for the mylar material. All subsequent flights were flown using this latter configuration. All flights were tracked with FPS-16 radars and exhibited excellent radar return.

ANALYSIS OF RESULTS

The 4.5-m-square Starutes displayed excellent stability, good fall rate characteristics, and were wind-sensitive at higher altitudes than hemispheric parachutes. As noted earlier, the 4.5-m diameter hemispheric parachute was subject to instabilities which caused telemetry signal dropouts and periodic oscillation in the temperature trace displayed on the strip chart recorder. Figure 11 shows a typical temperature trace with a hemispheric parachute and STS II rocketsonde. The effects of the unstable parachute are readily apparent in the frequent and intermittent telemetry dropouts. A strip chart recording of the temperature data telemetered from an STS II rocketsonde suspended from a Starute decelerator is shown in Figure 12. This figure shows a non-oscillating trace with very few data dropouts, demonstrating the advantage of utilizing the more stable decelerator.

On seven test flights the 1362-gram STS II rocketsonde was used as the payload. Combined with the Starute the ballistic coefficient, B , or M/C_dA , was 0.151 kg/m^2 . The ballistic coefficient of the 4.5-m diameter Arcas hemispheric parachute was calculated to be 0.268 kg/m^2 ; therefore, the fall rate was greater for the hemisphere parachute than for the Starute decelerator. The improved descent characteristics of the Starute over the hemispheric parachute are achieved by a combination of higher drag and lower decelerator weight. Figure 13 depicts the Starute and hemispheric parachute fall velocities with similar STS II payloads to demonstrate the more desirable descent characteristics of the Starute. There are significant differences in fall velocity at 65 km, as well as a 3-minute difference in descent times to 30-km altitude from apogee altitude of 65 km.

One flight was made using an STS II sonde with an additional 1452 grams of lead ballast. The purpose was to evaluate the performance of the 4.5-m-square

Starute with a heavier payload. In this test the Starute displayed excellent stability characteristics and the fall velocity was good, as shown in Figure 14. The ballistic coefficient for the Starute was calculated at 0.239 kg/m^2 ; the ballistic coefficient for the hemispheric parachute with this particular payload would have been 0.386 kg/m^2 .

As noted earlier, a decelerator is considered to be sensing winds when the fall velocity begins to decrease from its maximum value. Table 2 shows the selected wind sensitivity altitudes and corresponding fall velocities for each firing. The highest wind sensitivity altitude achieved was 72.4 km on 10 Nov 72. Three other flights were wind sensitive at 70 km or higher. Figure 15 is a theoretical evaluation of the performance of the 10 Nov 72 flight compared to the actual performance.* This comparison is useful because it will permit design decisions to be made when attempting to determine deployment altitudes required to measure winds at specified altitudes.

CONCLUSION

Tests of the 4.5-m-square Starute decelerator for meteorological sounding rocket applications have successfully demonstrated its improved stability, low ballistic coefficient as exhibited by its low fall velocity, and high altitude wind-sensing capability in comparison to the previously utilized hemispherical parachute. It also has exhibited good radar cross section and deployment reliability. These improved characteristics make the Starute a desirable decelerator for use with a wide variety of meteorological sounding payloads.

*As this figure indicates, the comparison between the theoretical and actual is in very good agreement.

REFERENCES

- 1) Meteorological Working Group, 1965, "The Meteorological Rocket Network IRIG," Document 111-64, Secretariat Range Commanders Council, White Sands Missile Range, New Mexico 88002.
- 2) Jenkins, K. R., 1962, "Empirical Comparisons of Meteorological Rocket Wind Sensors," J. Appl. Met., 1, 96-202.
- 3) Olsen, R. O., and G. Sloan., 1969, "An Improved Deceleration System for Upper Atmosphere Measurements," Proceedings Aerodynamic Deceleration System Conference, FTC-TR-69-H, El Centro, California.
- 4) Whitlock, C. H., and H. N. Murrow, 1964, "Performance Characteristics of a Preformed Elliptical Parachute at Altitudes Between 200,000 and 100,000 Feet Obtained by In-Flight Photography," NASA-TND-2183, Langley Research Center, Hampton, Virginia.
- 5) Graham, J. J., Jr., 1965, "Development of Ballute for Retardation of Arcas Rockersondes," Final Report Contract AF-19(628)-4149, Goodyear Aerospace Corp., Akron, Ohio.
- 6) Bollerman, B., 1970, "A Study of 30-km to 200-km Meteorological Rocket Sounding Systems," Vol. 1, Parts I and II, NASA-CR-1529, Marshall Space Flight Center, Huntsville, Alabama.
- 7) "Criteria for Determination of Reliability of Meteorological Rocket Data-ICAMRA/SAG/OWG," HQ 6th Weather Wing, Andrews AFB, MD, 1974.

TABLE 1
THE 4.5-M-SQUARE STARUTE MAJOR CHARACTERISTICS

Side Length	4.5 m
Material	1/4 mil Mylar (.006 mm)
Weight	1198 grams
Drag Area	21 m ²
Drag Coefficient	0.785
Height	3 m
Ram-Air Inlet Size	91.5 cm
Suspension Lines Length	61 cm

TABLE 2
4.5-M-SQUARE STARUTE SUMMARY CHART

Date	Payload	Payload Mass (gr)	Apogee (km)	Wind Sensitive Alt & Velocity (km, m/sec)	Notes
17 Sep 71	STS-II ¹	1362	61	49/70	135 second expulsion, Starute damaged by excessive heating during flight.
2 Nov 71	STS-II	1362	66	65/136	135 second expulsion, Satisfactory performance.
6 Mar 72	STS-II	1362	75	71/190	110 second expulsion, Satisfactory performance.
11 Oct 72	STS-II	1362	76	71/200	130 second expulsion, Satisfactory performance.
8 Nov 72	STS-II	1362	76	70/220	125 second expulsion, Satisfactory performance.
10 Nov 72	STS-II	1362	78	72/220	120 second expulsion, Satisfactory performance.
2 Feb 73	Ozone-sonde ²	2497	60	NA	145 second expulsion, Starute damaged by rocket motor at expulsion. Performance unsatisfactory.
12 Jul 73	STS-II	1362	68	66.5/138	110 second expulsion, Satisfactory performance.
17 Jul 73	MOD STS-II	2814	57	56/93	110 second expulsion, Satisfactory performance.
11 Jan 74	Gerdien ⁴	1400	70	69/200	135 second expulsion, Satisfactory performance.

¹Army stratosphere temperaturesonde

²Army ozone-measuring rocketsonde

³STS with ballast weight

⁴Payload designed to measure electron density

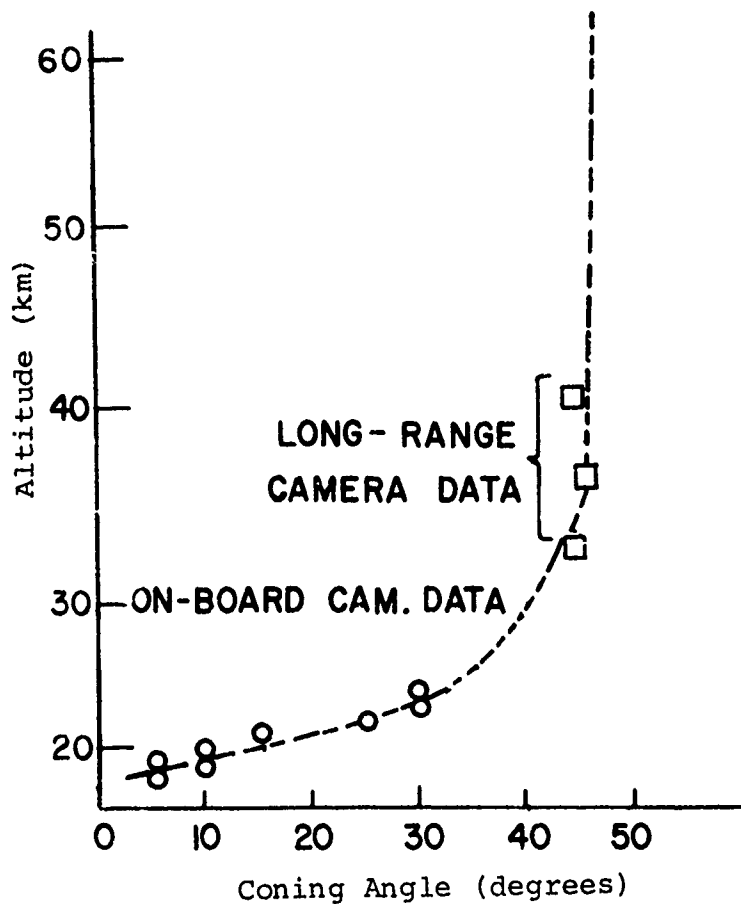


Figure 1. Coning angle variation with altitude for hemispherical silk parachutes.

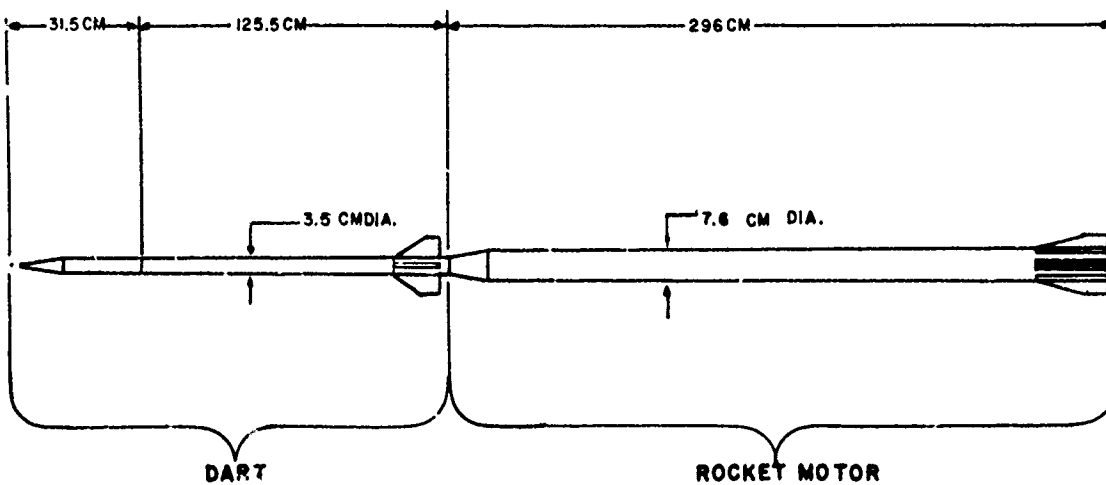


Figure 2. Loki dart vehicle configuration (assembled weight: 15.4 kg).

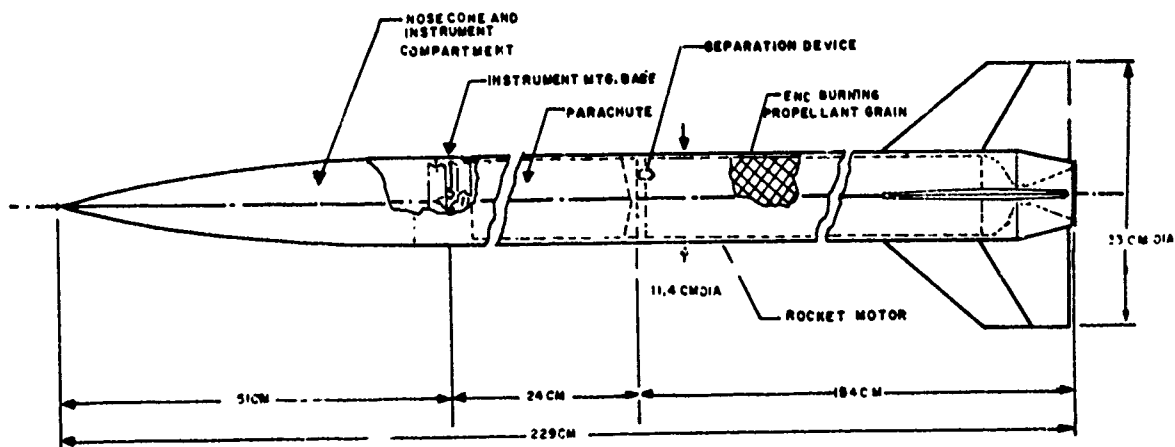


Figure 3. The Arcas vehicle configuration.

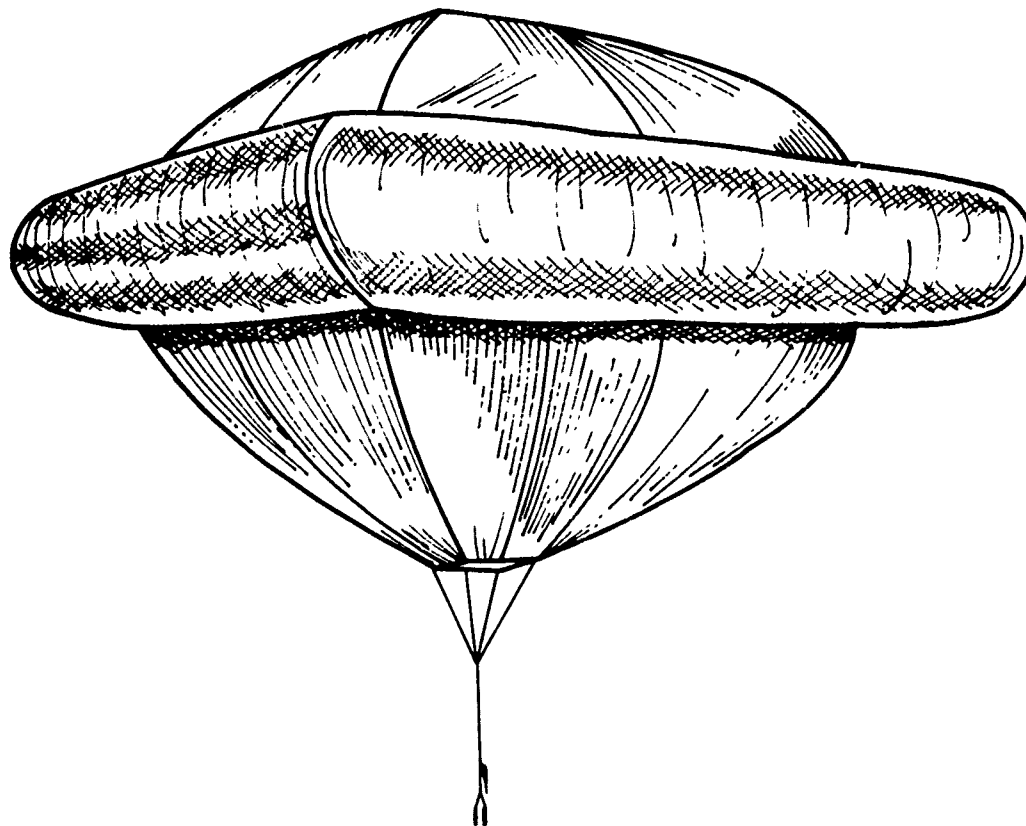


Figure 4. 4.5-m-square Starute configuration.

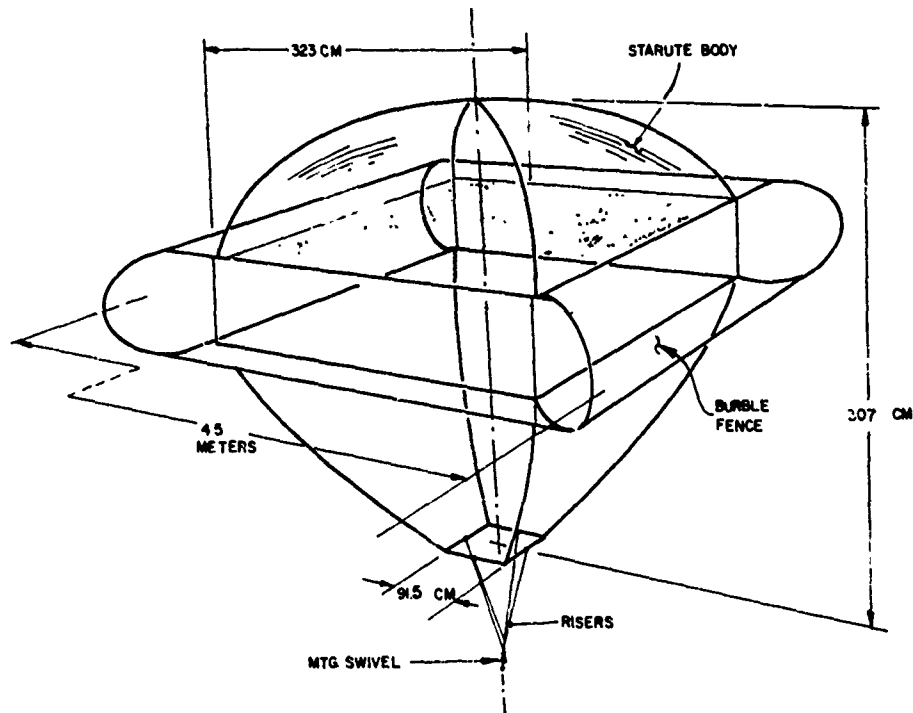


Figure 5. Major dimensions of Starute assembly.

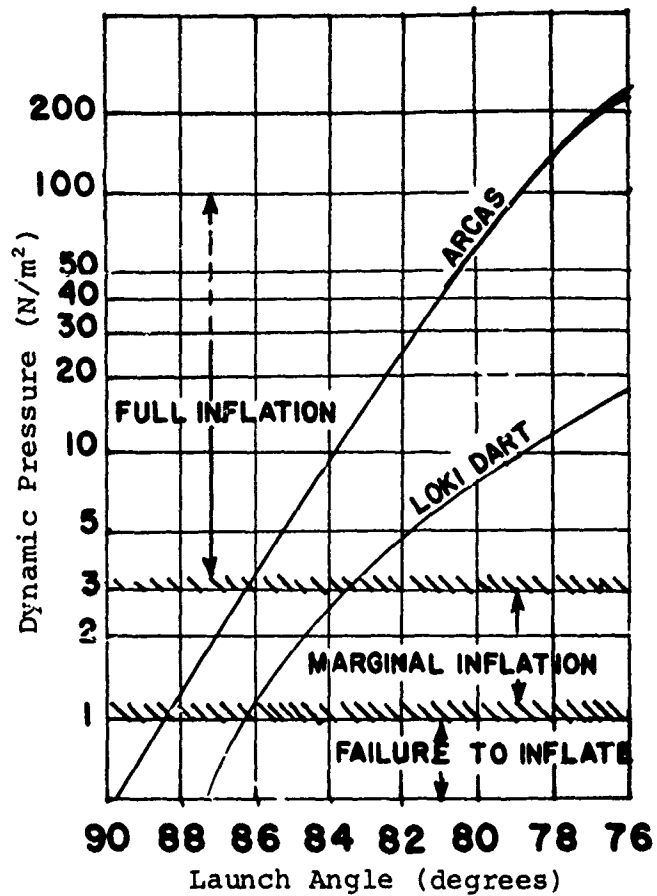


Figure 6. Dynamic pressure at apogee.

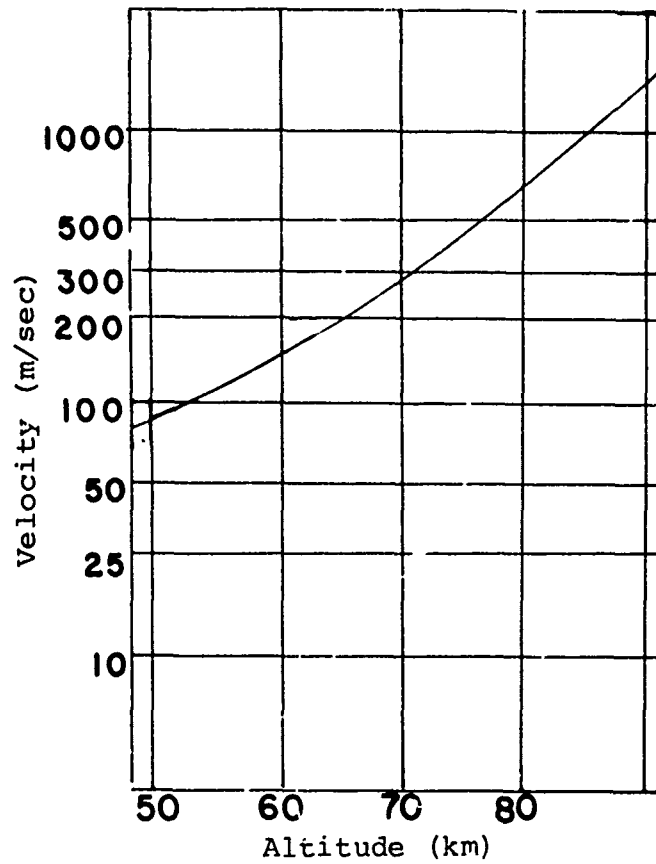


Figure 7. Critical velocity for parachute self-inflation (assuming critical inflation dynamic pressure of 3.4 N/m^2).

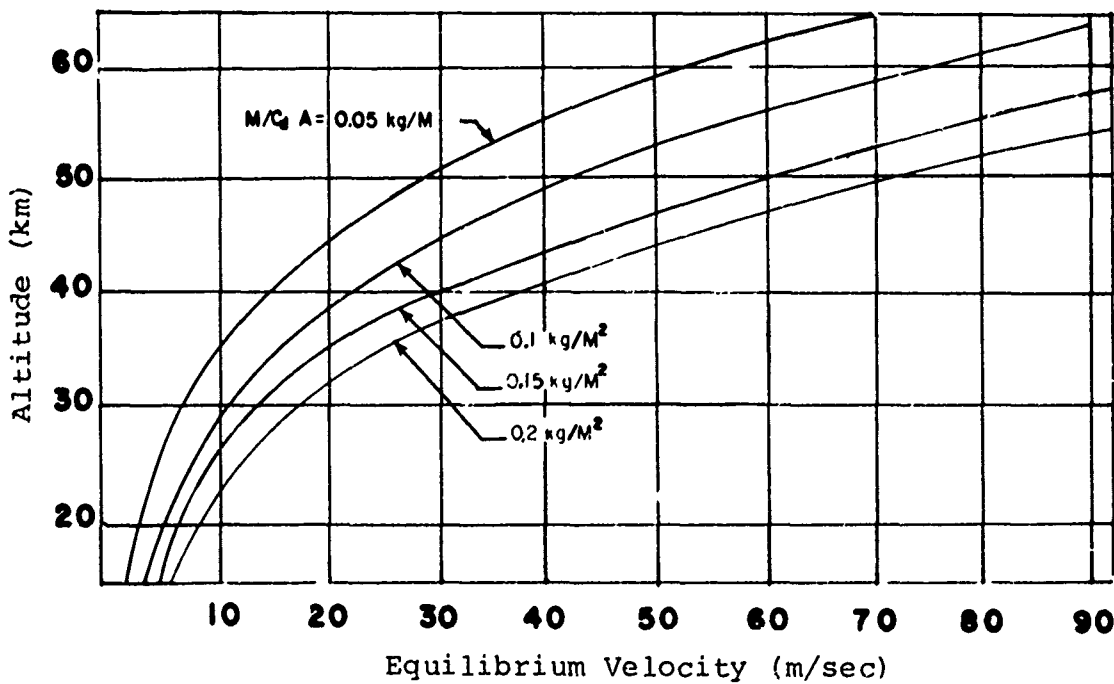


Figure 8. Velocity altitude profile various ballistic coefficients.

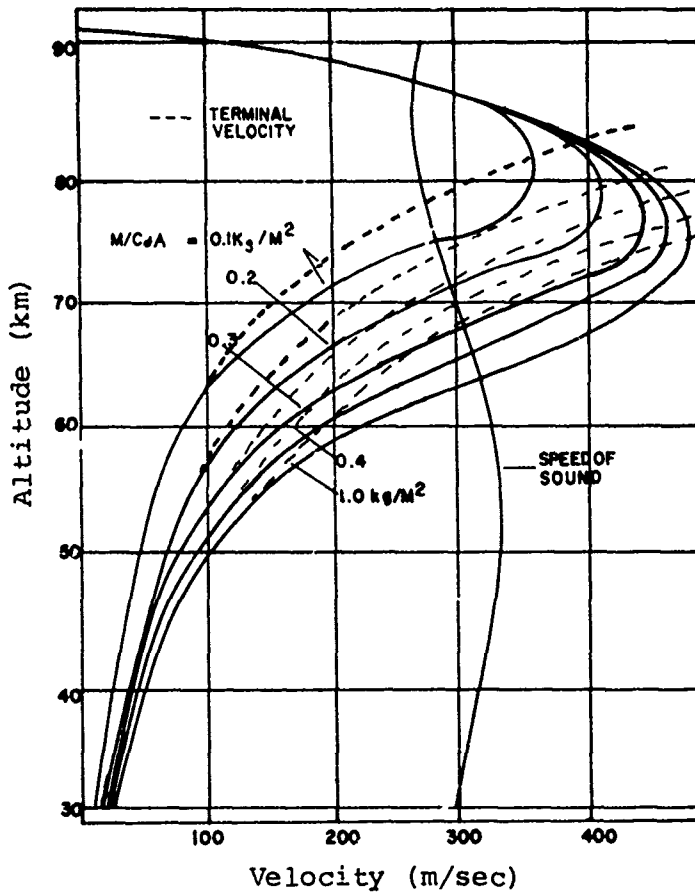


Figure 9. Altitude vs descent rate.

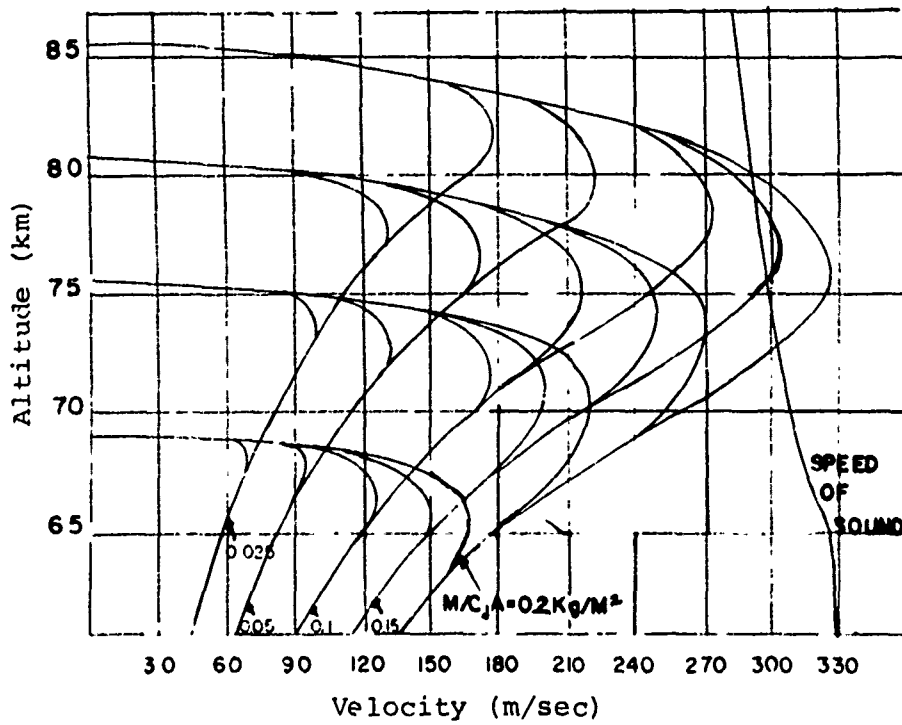


Figure 10. Descent curves from various release altitudes.

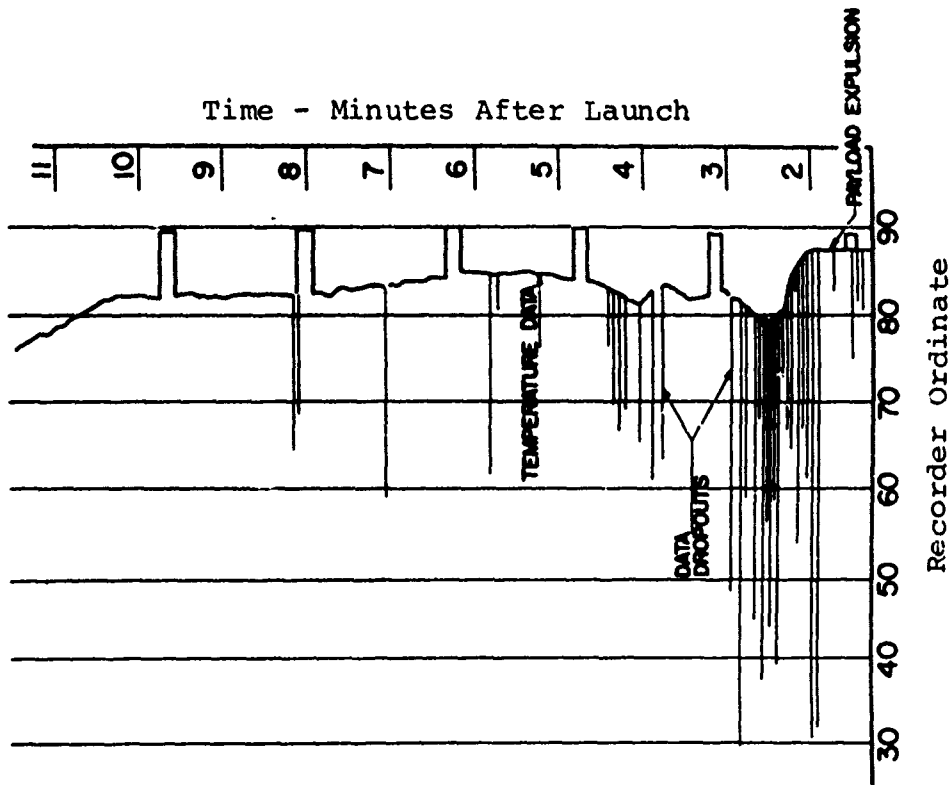


Figure 12. STS II Starute telemetry record, 12 Jul 73.

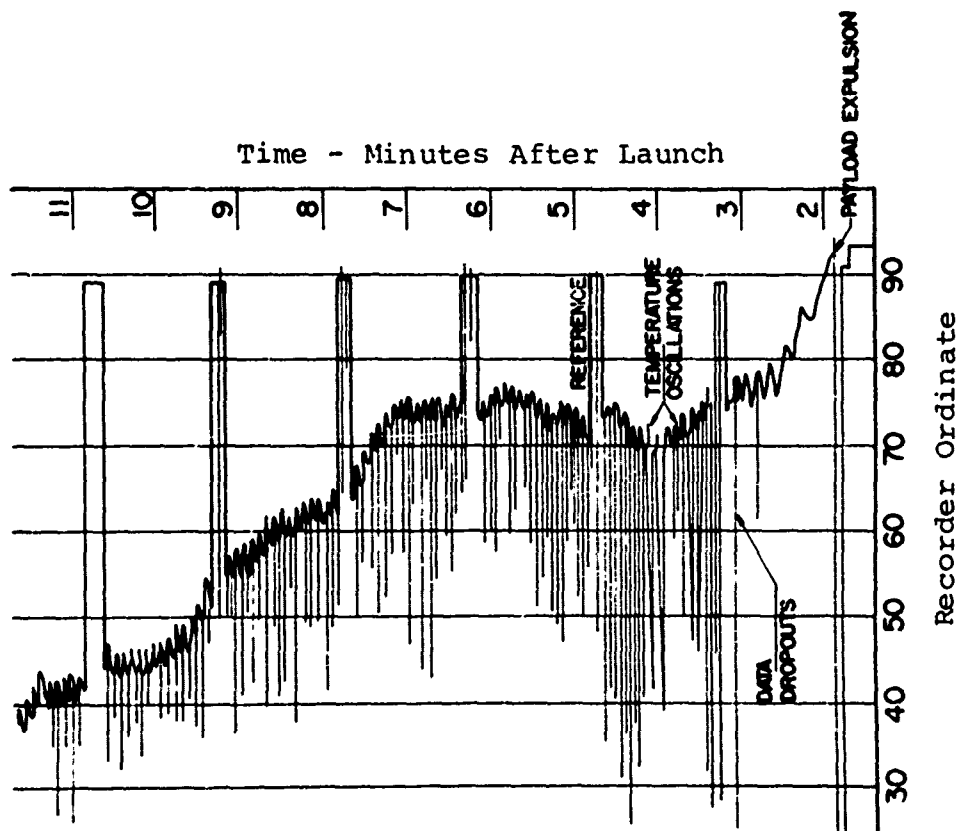


Figure 11. STS II hemisphere decelerator telemetry record, 3 Oct 72.

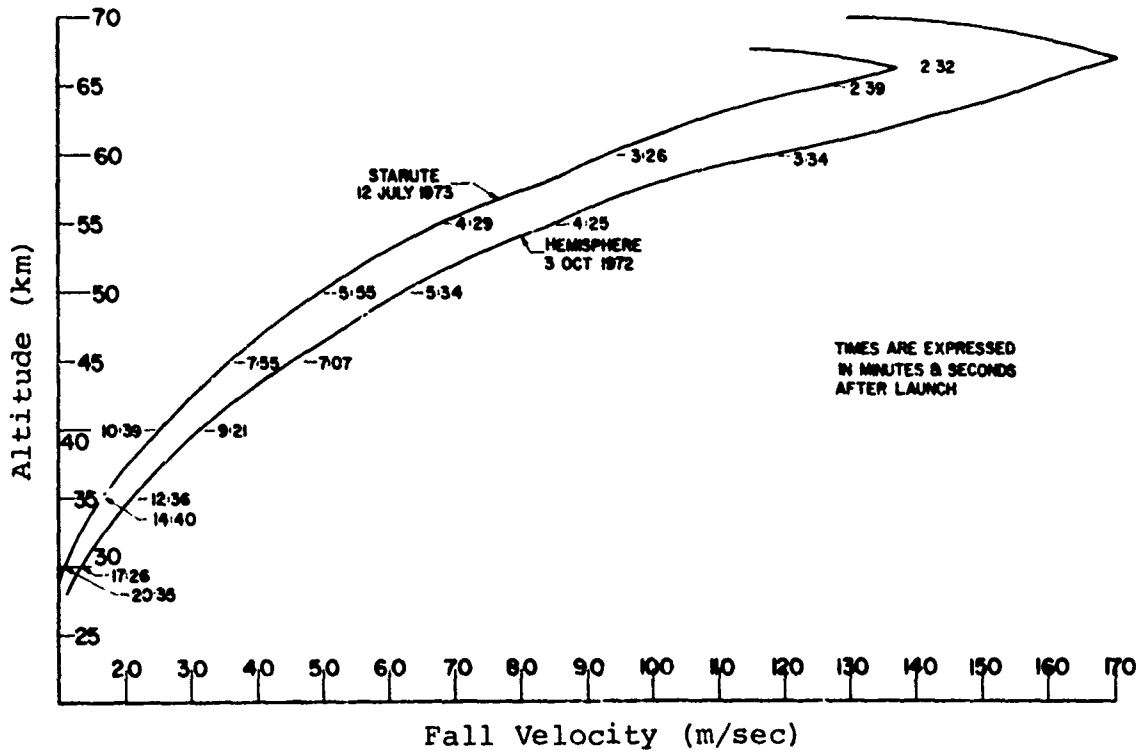


Figure 13. Fall rate of Starute and hemisphere parachute with an STS II payload.

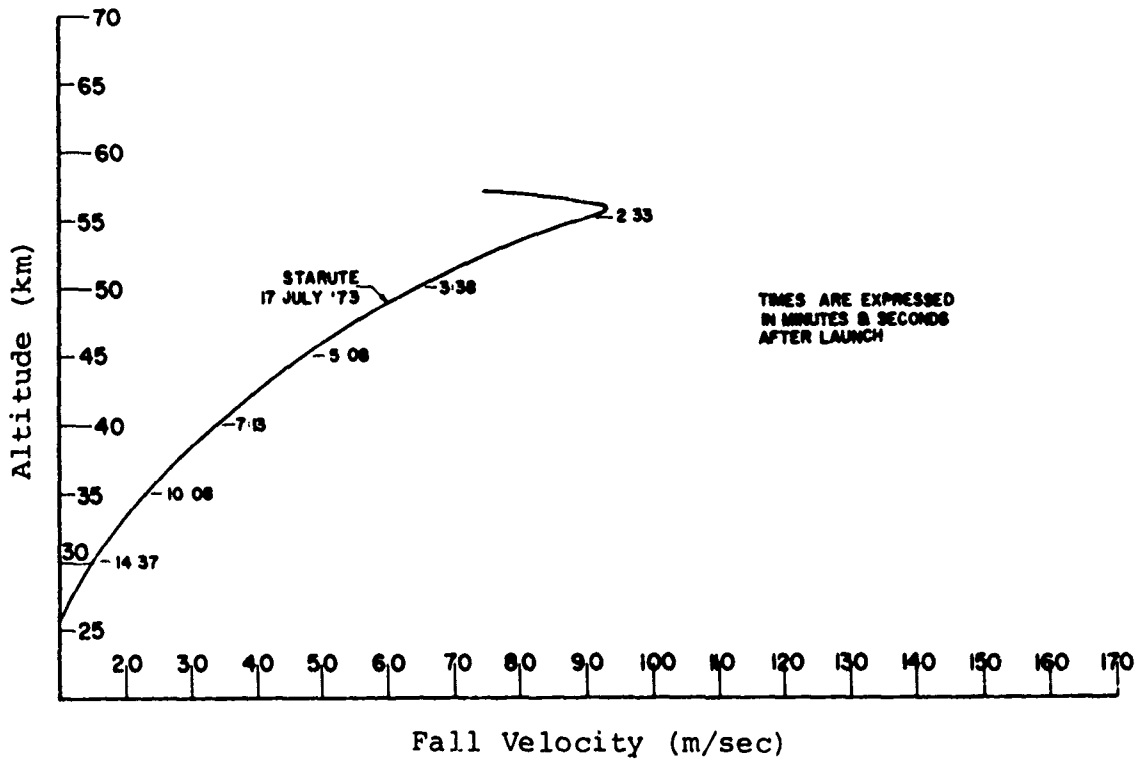


Figure 14. Fall rate of Starute with STS II payload.

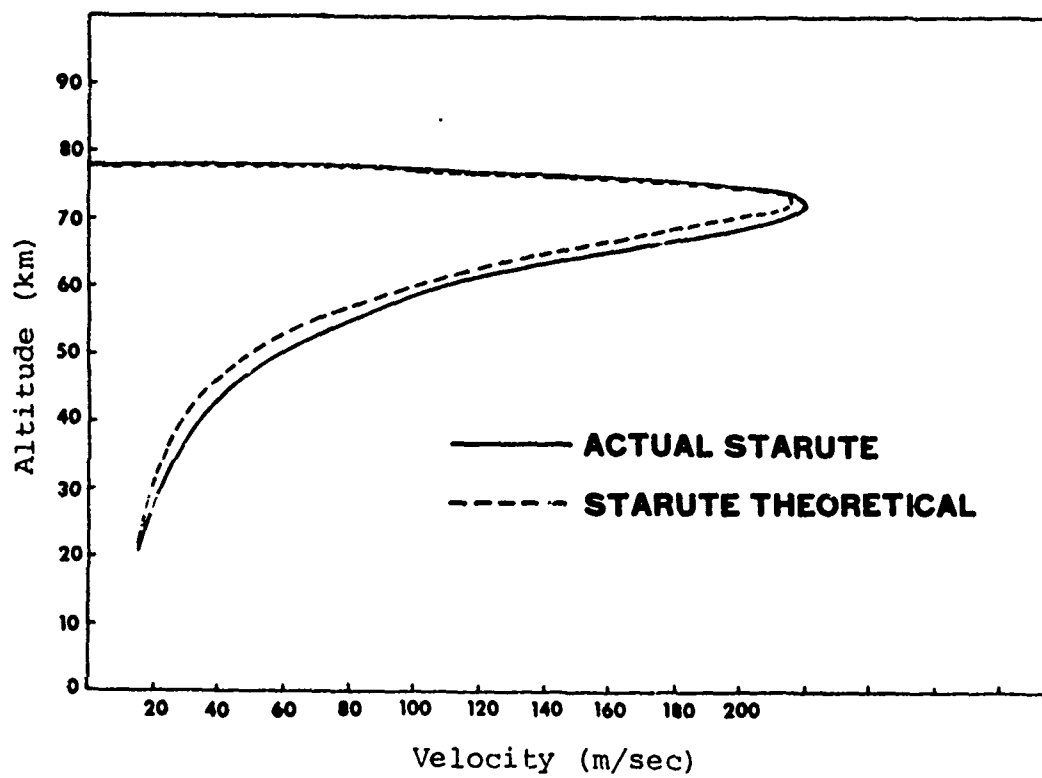


Figure 15. Theoretical and actual fall rate of Starute with 2.6 kg payload.

ATMOSPHERIC SCIENCES RESEARCH PAPERS

1. White, Kenneth O., James B. Gillespie, Robert Armstrong, and Larry E. Traylor, "State-of-the-Art Survey of Meteorological Instrumentation Required to Determine Atmospheric Effects on Airborne Laser Tests," ECOM-5469, January 1973.
2. Duncan, Louis D., and Barbara J. Richart, "Mesoscale Variation of Spectral Radiance Near 15 Micrometers," ECOM-5470, January 1973.
3. Schleusener, Stuart A., and Kenneth O. White, "Solid-State Laser Multiwavelength Identification and Display System," ECOM-5473, January 1973.
4. Nordquist, Walter S., Jr., "Numerical Approximations of Selected Meteorological Parameters Related to Cloud Physics," ECOM-5475, March 1973.
5. Maynard, Harry, "An Evaluation of Ten Fast Fourier Transform (FFT) Programs," ECOM-5476, March 1973.
6. Gerber, Hermann E., "Freezing Water with Sized AgI Particles. I: A Survey," ECOM-5477, March 1973.
7. Gerber, Hermann E., "Freezing Water with Sized AgI Particles. II: Theoretical Considerations," ECOM-5478, March 1973.
8. D'Arcy, Edward M., "Accuracy Study of the T-9 Radar," ECOM-5480, March 1973.
9. Miller, Walter B., "An Investigation of Errors Introduced into Meteorological Calculations Through Use of the Hypsometric Equation," ECOM-5481, April 1973.
10. Miller, Walter B., "On Indirect Pressure Estimation from Measurements of Height and Temperature," ECOM-5482, April 1973.
11. Rinehart, G. S., and R. P. Lee, "Apparent 7-Day Period in Visibility Data at White Sands Missile Range, New Mexico," ECOM-5484, April 1973.
12. Swingle, Donald M., and Raymond Bellucci, "Improved Sound Ranging Location of Enemy Artillery," ECOM-5486, April 1973.
13. Lindberg, James D., and David G. Snyder, "Determination of the Optical Absorption Coefficient of Powdered Materials Whose Particle Size Distribution and Refractive Indices Are Not Known," ECOM-5487, April 1973.
14. Rubio, Roberto, "Winter Anomalous Radio Wave Absorption Days at 32°N Latitude and Prevalent Solar Radiation," ECOM-5488, May 1973.
15. Nordquist, W. S., "Data from a Fog Dispersal Experiment Using Helicopter Downwash," ECOM-5456, May 1973.
16. Shinn, Joseph H., "Optimum Wind Soundings and Army Fallout Prediction Accuracies," ECOM-5489, May 1973.
17. Miller, Walter B., and Donald R. Veazey, "An Integrated Error Description of Active and Passive Balloon Tracking Systems," ECOM-5500, June 1973.
18. Doll, Barry, "The Potential Use of Polarized Reflected Light in the Remote Sensing of Soil Moisture," ECOM-5501, July 1973.
19. Duncan, Louis D., "A Geometric Investigation of the Effect of Viewing Angle on the Ground Resolution of Satellite-Borne Sensors," ECOM-5502, July 1973.
20. Miller, Walter B., and Donald R. Veazey, "Vertical Efficiency of Active and Passive Balloon Tracking Systems from a Standpoint of Integrated Error," ECOM-5503, July 1973.
21. Richter, Thomas J., "Design Considerations for the Calculator, Altitude ML-646(XE-1)/UM," ECOM-5504, August 1973.
22. Randhawa, J. S., "Measurement of Total Ozone at WSMR, NM," ECOM-5505, August 1973.
23. Mason, James B., "Lidar Measurement of Temperature: A New Approach," ECOM-5506, August 1973.
24. Randhawa, J. S., "An Investigation of Solar Eclipse Effect on the Subpolar Stratosphere," ECOM-5507, September 1973.
25. Wade, Gerald T., Teddy L. Barber, and Robert Armstrong, "A Proposed Versatile Photon Counter System for Laser Radar," ECOM-5508, September 1973.
26. Lentz, W. J., "A New Method of Computing Spherical Bessel Functions of Complex Argument with Tables," ECOM-5509, September 1973.

27. White, Kenneth O., Gerald T. Wade, and Stuart A. Schleusener, "The Application of Minicomputers in Laser Atmospheric Experiments," ECOM-5510, September 1973.
28. Collett, E., R. Alferness, and T. Forbes, "Log-Intensity Correlations of a Laser Beam in a Turbulent Medium," ECOM-5511, September 1973.
29. Robbiani, Raymond L., "Design Concept of a Forward Area Rawinsonde Set (FARS)," ECOM-5512, October 1973.
30. Stone, William J., "The Hydrometeorologic Ground Truth Facility at White Sands Missile Range, New Mexico," ECOM-5513, October 1973.
31. Lacy, Claud H., "Objective Analysis Using Modeled Space-Time Covariances: An Evaluation," ECOM-5514, October 1973.
32. Stipanuk, G. S., "Algorithms for Generating a SKEW-T, log p DIAGRAM and Computing Selected Meteorological Quantities," ECOM-5515, October 1973.
33. Sharenow, Moses, "Test and Evaluation of Natural Rubber Spherical Balloons," ECOM-5516, October 1973.
34. White, Kenneth O., and Gerald T. Wade, "Remote Sensing of Atmospheric Methane Using an Erbium/YAG Laser: A Feasibility Study," ECOM-5517, October 1973.
35. Tchen, Chan Mou, and Edward Collett, "The Spectrum of Laser-Induced Turbulence," ECOM-5518, February 1974.
36. Collett, Edward, and Chan Mou Tchen, "Turbulent Heating of an Atmosphere by a Laser Beam," ECOM-5519, February 1974.
37. Gerber, Hermann E., "Freezing Water with Sized AgI Particles. III: Experimental Procedure, Results, and Conclusions," ECOM-5520, March 1974.
38. Lindberg, James D., "A Simple Method for Measuring Absolute Diffuse Reflectance with a Laboratory Spectrophotometer," ECOM-5521, November 1973.
39. Lindberg, James D., and Michael S. Smith, "Visible and Near Infrared Absorption Coefficients of Kaolinite and Related Clays," ECOM-5522, November 1973.
40. Weathers, L. R., and R. B. Loveland, "Magnetic Field Survey at White Sands Missile Range, New Mexico," ECOM-5523, November 1973.
41. Matonis, Casimir J., "The Potential Use of Tactical Microwave Radio (TMR) for Transmission of Weather Radar Data," ECOM-5524, December 1973.
42. Lindberg, James D., and Larry S. Laude, "A Measurement of the Absorption Coefficient of Atmospheric Dust," ECOM-5525, December 1973.
43. Low, Richard D. H., "Microphysical and Meteorological Measurements of Fog Supersaturation," ECOM-5526, December 1973.
44. Nordquist, Walter S., "Fog Clearing Using Helicopter Downdrafts: A Numerical Model," ECOM-5527, December 1973.
45. Lentz, W. J., and G. B. Hoidale, "Estimates of the Extinction of Electromagnetic Energy in the 8 to 12 μ m Range by Natural Atmospheric Particulate Matter," ECOM-5528, January 1974.
46. Duncan, Louis D., and Marvin Kays, "Determining Nuclear Fallout Winds from Satellite-Observed Spectral Radiances," ECOM-5529, January 1974.
47. Henley, David C., "An Analysis of Random Fluctuations of Atmospheric Dust Concentrations," ECOM-5530, January 1974.
48. Gillespie, James B., and Carmine Petracca, "Atmospheric Effects for Ground Target Signature Modeling. II. Discussion and Application of a Generalized Molecular Absorption Model," ECOM-5531, January 1974.
49. Anthes, Richard A., and Thomas T. Warner, "Prediction of Mesoscale Flows Over Complex Terrain," ECOM-5532, March 1974.
50. Low, Richard D. H., "Microphysical Evolution of Fog," ECOM-5533, March 1974.
51. Duncan, Louis D., "An Iterative Inversion of the Radiative Transfer Equation for Temperature Profiles," ECOM-5534, March 1974.
52. Blanco, A. J., E. M. D'Arcy, and J. B. Gillespie, "Degradation of a Helium-Neon Laser Beam by Atmospheric Dust During a Sand Storm," ECOM-5535, March 1974.
53. Barr, William C., "An Analysis of Loran Wind-Measuring Accuracies for Application to Field Army Use," ECOM-5536, April 1974.
54. Westwater, E. R., J. B. Snider, A. V. Carlson, and J. R. Yoder, "Experimental Determination of Temperature Profiles by Ground-Based Radiometry," ECOM-5537, April 1974.

55. White, Kenneth O., W. R. Watkins, and S. A. Schleusener, "Measurement of Ho^{1+} :YLF 2.06 μm Laser Spectral Output Variations and CO_2 Absorption Coincidence," ECOM-5538, April 1974.
56. Gillespie, James B., James D. Lindberg, and Michael S. Smith, "Visible and Near-Infrared Absorption Coefficients of Montmorillonite and Related Clays," ECOM-5539, May 1974.
57. Cantor, Israel, "Aerosol Angular Scattering Functions for Model Atmospheres," ECOM-5540, May 1974.
58. Pena, Ricardo, and H. N. Schwartz, "A High Resolution Temperature Sonde for the Lower Atmosphere," ECOM-5541, May 1974.
59. Diderich, Robert A., Kenneth M. Barnett, and Ronald M. Cionco, "Evaluation of Several Wire Mesh Screens for the Protection and Ventilation of Meteorological Sensors," ECOM-5542, May 1974.
60. Miller, Walter B., and Donald R. Veazey, "On Increasing Vertical Efficiency of a Passive Balloon Tracking Device by Optimal Choice of Release Point," ECOM-5543, June 1974.
61. Randhawa, J. S., "Partial Solar Eclipse Effects on Temperature and Wind in an Equatorial Atmosphere," ECOM-5544, June 1974.
62. Duncan, Louis D., "Approximations in Inverting the Radiative Transfer Equation," ECOM-5545, July 1974.
63. Pries, Thomas H., and Erick T. Young, "Evaluation of a Laser Crosswind System," ECOM-5546, July 1974.
64. Shinn, Joseph H., and Harry W. Maynard, "On the Sensitivity of Selected Typical Tactical Army Operations to Weather Effects," ECOM-5547, October 1974.
65. Miller, Walter, and Bernard Engebos, "On Determining Cost-Effectiveness of an Army Automatic Meteorological System," ECOM-5548, November 1974.
66. Conover, Walter, "Operational Techniques for Radar Set AN/TPS-41," ECOM-5549, November 1974.
67. Barber, T. L., and J. B. Mason, "A Transit-Time Lidar Wind Measurement: A Feasibility Study," ECOM-5550, December 1974.
68. Olsen, R. O., and B. W. Kennedy, "The Utilization of Starute Decelerators for Improved Upper Atmosphere Measurements," ECOM-5551, December 1974.